Mappings between Sphere, Disc, and Square

Martin Lambers
University of Siegen, Germany

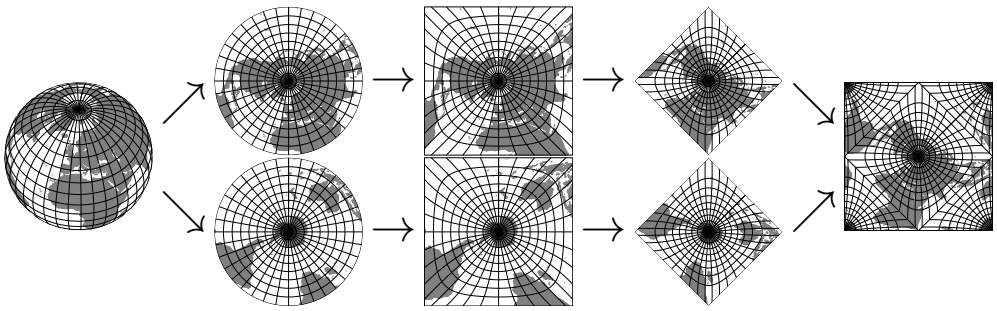

Figure 1. A mapping between a sphere and a square, composed of a mapping between a hemisphere and a disc, a mapping between a disc and a square, and an arrangement of two squares in a new square.

Abstract

A variety of mappings between a sphere and a disc and between a disc and a square, as well as combinations of both, are used in computer graphics applications, resulting in mappings between spheres and squares. Many options exist for each type of mapping; to pick the right methods for a given application requires knowledge about the nature and magnitude of mapping distortions.

This paper provides an overview of forward and inverse mappings between a unit sphere, a unit disc, and a unit square. Quality measurements relevant for computer graphics applications are derived from tools used in the field of map projection, and a comparative analysis of the mapping methods is given.

1. Introduction and Background

Mappings between spheres, discs, and squares are useful tools in many areas of computer graphics. Examples include panoramic imaging [German et al. 2007; Fong 2014], environment mapping [Greene 1986; Heidrich and Seidel 1998], and generating points on a disc or sphere for sampling purposes [Shirley and Chiu 1997; Sloan et al. 2005].

 ISSN 2331-7418

Important properties of such mappings include the angle and area distortions that they introduce [Floater and Hormann 2005]. Some applications require equal-area mappings that preserve area ratios, and others require conformal mappings that preserve angles locally. No mapping can be both equal-area and conformal at the same time, and preserving one quality often results in strong distortions in the other. Many applications, in particular in computer graphics, require mappings that allow efficient sampling of maps [Snyder and Mitchell 2001] without introducing artifacts. A balanced mapping for this purpose provides both small area distortions and small angle distortions, although neither distortion has to be zero.

This paper gives an overview of mappings between a unit sphere, a unit disc, and a unit square, with formulas for forward and inverse transformation. Furthermore, we derive two quality measurements relevant for computer graphics applications based on established tools from the field of map projection, and we compare the mappings based on these measurements.

Section 2 starts with mappings between discs and squares, Section 3 describes map projections between spheres (or hemispheres) and discs, and Section 4 details methods to combine methods from both categories to produce mappings between spheres and squares. Section 5 provides numerical analysis results for all mappings based on the derived quality measurements. The supplementary material consists of C++ source code that implements all mapping and analysis methods as well as all tools necessary to recreate the figures and results presented in this paper.

2. Mappings between Disc and Square

This section provides an overview of mappings between the closed unit disc D and the closed unit square R. We identify points on D using either polar coordinates, with radius r and angle φ, $0 \leq r \leq 1$, $-\pi < \varphi \leq \pi$, or Cartesian coordinates, u and v with $r = \sqrt{u^2 + v^2}$ and $\varphi = \operatorname{atan2}(v, u)$. Points on R are identified using Cartesian coordinates x and y, $-1 \leq x \leq +1$, $-1 \leq y \leq +1$. The mappings are summarized and compared in Table 1.

2.1. Radial Stretching

Perhaps, the most direct method of mapping a disc to a square is to adjust the radius of a point on the disc according to its angle.

For $(x, y) \in R$, we have a distance of $t = \sqrt{x^2 + y^2}$ to the origin and a polar angle of $\varphi = \operatorname{atan2}(y, x)$. The polar radius of $(r, \varphi) \in D$ can then be set to $r = t \cos\varphi$ for $\varphi \in [-\pi/4, +\pi/4]$ (and accordingly for the remaining ranges of φ). Using $\cos\varphi = x/t$, $\sin\varphi = y/t$, $\tan\varphi = v/u$, and a method applied by Cline to Shirley's equal-area mapping [Shirley and Cline 2011] to reduce the number of cases, this leads to the following simple equations (see the derivation by Fong for details [Fong 2015]):

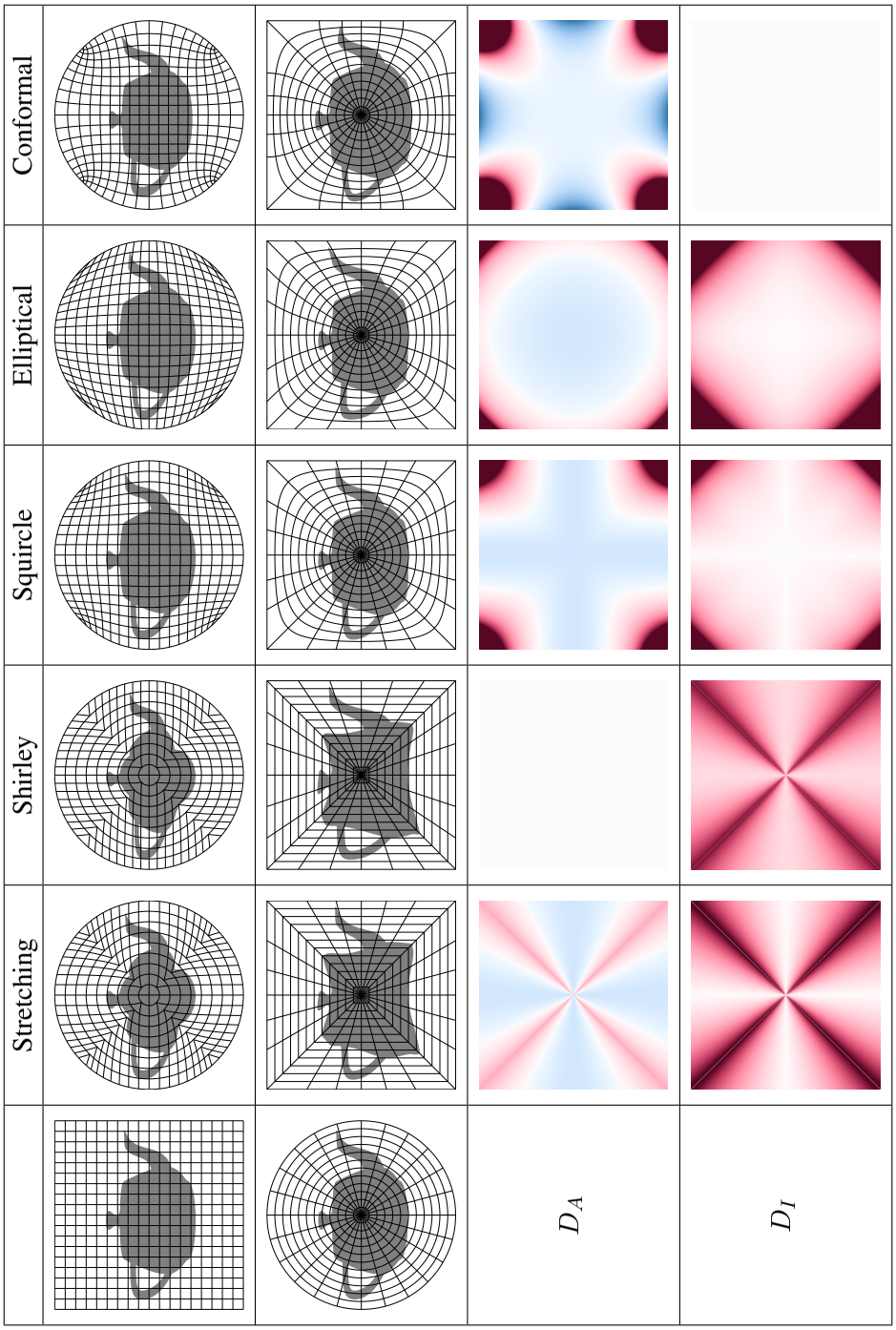

Table 1. Overview of mappings between a disc and a square.

Disc to square mapping:

$$r = \sqrt{u^2 + v^2}$$

$$(x, y) = \begin{cases} (0, 0) & \text{if } r = 0 \\ (\text{sgn}(u) \cdot r, \text{sgn}(v) \cdot rv/u) & \text{if } r > 0 \text{ and } u^2 \geq v^2 \\ (\text{sgn}(u) \cdot ru/v, \text{sgn}(v) \cdot r) & \text{if } r > 0 \text{ and } u^2 < v^2 \end{cases}$$

Square to disc mapping:

$$t = \sqrt{x^2 + y^2}$$

$$(u, v) = \begin{cases} (0, 0) & \text{if } t = 0 \\ (\text{sgn}(x) \cdot x^2/t, \text{sgn}(y) \cdot xy/t) & \text{if } t > 0 \text{ and } x^2 \geq y^2 \\ (\text{sgn}(x) \cdot xy/t, \text{sgn}(y) \cdot y^2/t) & \text{if } t > 0 \text{ and } x^2 < y^2 \end{cases}$$

This mapping is neither conformal nor equal-area. It suffers from strong angular and area distortions.

2.2. Shirley's Equal-Area Mapping

Shirley constructs an equal-area map between a disc and a square by mapping concentric disc strings to concentric square strips [Shirley and Chiu 1997]. Note that Roşca derived an equivalent mapping (except for a scale factor) using a different approach [Roşca 2010]. Both prove the equal-area property by showing that the Jacobian is constant. The following formulas for the disc-to-square mapping are based on Shirley's code samples. The formulas for the inverse mapping are based on Cline's method for reducing the number of cases [Shirley and Cline 2011].

Disc to square mapping:

$$r = \sqrt{u^2 + v^2}$$

$$\varphi = \begin{cases} \text{atan2}(v, u) & \text{if } \text{atan2}(v, u) \geq -\pi/4 \\ \text{atan2}(v, u) + 2\pi, & \text{otherwise} \end{cases}$$

$$(x, y) = \begin{cases} (r, \frac{4}{\pi} r\varphi) & \text{if } \varphi < \pi/4 \\ (-\frac{4}{\pi} r(\varphi - \pi/2), r) & \text{if } \varphi < 3\pi/4 \\ (-r, -\frac{4}{\pi} r(\varphi - \pi)) & \text{if } \varphi < 5\pi/4 \\ (\frac{4}{\pi} r(\varphi - 3\pi/2), -r), & \text{otherwise} \end{cases}$$

Square to disc mapping:

$$(r, \varphi) = \begin{cases} (x, \frac{\pi}{4} y/x) & \text{if } x^2 > y^2 \\ (y, \frac{\pi}{2} - \frac{\pi}{4} x/y) & \text{if } x^2 \leq y^2 \text{ and } y^2 > 0 \\ (0, 0), & \text{otherwise} \end{cases}$$

Note that by writing the square to disc mapping of the radial stretching method in terms of r, φ, using $\cos\varphi = x/t$ and $\sin\varphi = y/t$, one can see that Shirley's mapping uses the same stretching of the radius but modifies the angle, φ.

This mapping is equal-area. It suffers from strong angular distortions, especially around the discontinuities at the diagonals of the square.

2.3. Fernández-Guasti's Squircle Mapping

Fernández-Guasti introduced a geometric form that can be varied between square and circle using a "squareness" parameter [Fernández-Guasti 1992]; he later called this form squircle. Note that the term squircle is sometimes used to refer to a special case of a superellipse. To avoid ambiguities, we therefore use the term "Fernández-Guasti's squircle".

In terms of Cartesian coordinates, the equation that describes Fernández-Guasti's squircle is $\frac{s^2}{k^4}x^2y^2 - \frac{x^2+y^2}{k^2} + 1 = 0$, where s is the squareness parameter and k is the radius of the circle (for $s = 0$) or half the side length of the square (for $s = 1$). For values of s between 0 and 1, the geometry resembles both square and circle.

Fong proposes to map concentric circles to concentric squircles to construct a mapping between a unit disc and a unit square [Fong 2014]. For this purpose, he sets $s = k$ and varies s from 0 to 1, taking $r = s = \sqrt{x^2 + y^2 - x^2y^2}$ as disc radius.

Disc to square mapping:

$$w = \frac{\operatorname{sgn}(uv)}{\sqrt{2}}\sqrt{u^2 + v^2 - \sqrt{(u^2 + v^2)(u^2 + v^2 - 4u^2v^2)}}$$

$$(x, y) = \begin{cases} (w/v, w/u) & \text{if } |w| > 0 \\ (u, v), & \text{otherwise} \end{cases}$$

Square to disc mapping:

$$u = x\frac{\sqrt{x^2 + y^2 - x^2y^2}}{\sqrt{x^2 + y^2}}$$

$$v = y\frac{\sqrt{x^2 + y^2 - x^2y^2}}{\sqrt{x^2 + y^2}}$$

Note that $(0, 0)$ must be mapped to $(0, 0)$ as a special case.

This mapping is neither equal-area nor conformal.

2.4. Elliptical Arc Mapping

Nowell derived a method to map a square to a disc by mapping lines of constant x and lines of constant y in the square to ellipses in the disc [Nowell 2005]. Cigolle et al. mention an elliptical mapping between a disc and a square [Cigolle et al. 2014]. Their paper omits details, but their implementation in the supplementary material

shows that they derived equivalent formulas for the mapping from square to disc and additional formulas for the inverse mapping. The simpler formulas for the inverse mapping given below were derived by Fong [Fong 2015].

Disc to square mapping:

$$x = \frac{1}{2}\sqrt{2 + u^2 - v^2 + 2\sqrt{2}u} - \frac{1}{2}\sqrt{2 + u^2 - v^2 - 2\sqrt{2}u}$$
$$y = \frac{1}{2}\sqrt{2 - u^2 + v^2 + 2\sqrt{2}v} - \frac{1}{2}\sqrt{2 - u^2 + v^2 - 2\sqrt{2}v}$$

Square to disc mapping:

$$u = x\sqrt{1 - \frac{y^2}{2}}$$
$$v = y\sqrt{1 - \frac{x^2}{2}}$$

This mapping is neither equal-area nor conformal.

2.5. Conformal Mapping

In complex analysis, the Schwarz-Christoffel transformation provides a way to construct conformal transformations between simple polygons and the upper half of the complex plane. Since there exists a conformal transformation between the upper half of the complex plane and the open unit disc, one can construct a conformal mapping between a square and a disc. Indeed, this special case was used as illustration and motivation in Schwarz' original publication on the topic. However, formulas for forward and inverse mappings suitable for implementation on computers were not available for some time.

Conformal mapping of a disc onto a rotated square using the Schwarz-Christoffel transformation is a core element of the Peirce quincuncial map projection [Peirce 1879]; see also Section 4. The formulas given below are based on Lee's analysis of Peirce's projection [Lee 1976].

The mapping from disc to square first rotates the disc by $45°$. This step is not necessary, but it makes this mapping consistent with the others with regard to the orientation of the square content. Then, the rotated disc is conformally mapped to a rotated square with corners $(1, 0)$, $(0, 1)$, $(-1, 0)$, $(0, -1)$. This square is then rotated and scaled to fit the unit square. The conformal mapping is based on the incomplete elliptic Legendre integral, F, with a modulus of $k = 1/\sqrt{2}$. This integral must be computed using iterative methods. Numerical libraries usually provide the necessary methods; our supplementary material includes an implementation based on the Landen transformation.

The mapping from square to disc first rotates and scales the unit square back into the square with corners $(1, 0)$, $(0, 1)$, $(-1, 0)$, $(0, -1)$. It then uses the complex-valued Jacobian elliptic function cn with modulus $k = 1/\sqrt{2}$ to conformally map

that square to the unit circle. Afterwards, the inverse of the optional rotation is applied. This mapping requires the value $K = F(\pi/2) \approx 1.854$, which is the complete elliptic integral of the first kind with modulus $k = 1/\sqrt{2}$. The function cn must again be computed using iterative methods. Numerical libraries often provide real-valued implementations that compute the related functions cn, sn, and dn at the same time; our supplementary material includes an implementation based on the arithmetic-geometric mean. For the special case of $k = 1/\sqrt{2}$, the complementary elliptic modulus $k' = \sqrt{1-k^2}$ is identical to k, and the complex cn function can be computed from real-valued cn, sn, and dn as follows:

$$\mathrm{cn}(x+iy) = \frac{\mathrm{cn}(x)\,\mathrm{cn}(y)}{1-\mathrm{dn}^2(x)\,\mathrm{sn}^2(y)} - i\frac{\mathrm{sn}(x)\,\mathrm{dn}(x)\,\mathrm{sn}(y)\,\mathrm{dn}(y)}{1-\mathrm{dn}^2(x)\,\mathrm{sn}^2(y)}$$

Note that Stark derives optimized numerical methods for the special case of conformal mappings between unit sphere and unit disc [Stark 2009].

Disc to square mapping:

$$\begin{aligned}
u' &= (u-v)/\sqrt{2} \\
v' &= (u+v)/\sqrt{2} \\
A &= u'^2 + v'^2 \\
B &= u'^2 - v'^2 \\
T &= \sqrt{(1+A^2)^2 - 4B^2} \\
U &= 1 + 2B - A^2 \\
\alpha &= \mathrm{acos}((2A-T)/U) \\
\beta &= \mathrm{acos}(U/(2A+T)) \\
x' &= \mathrm{sgn}(u')(1 - F(\alpha)/2K) \\
y' &= \mathrm{sgn}(v')(F(\beta)/2K) \\
x &= x' + y' \\
y &= y' - x'
\end{aligned}$$

Square to disc mapping:

$$\begin{aligned}
x' &= x/2 - y/2 \\
y' &= x/2 + y/2 \\
w &= \mathrm{cn}(K(1-x') - iKy') \\
u &= (\Re(w) + \Im(w))/\sqrt{2} \\
v &= (\Im(w) - \Re(w))/\sqrt{2}
\end{aligned}$$

This mapping is conformal, except for the four singular points located on the corners of the square. Area deformation is substantial, especially near the singular points.

3. Mappings between Sphere and Disc

This section covers mappings between the unit sphere, S, and the unit disc, D. We identify points on S using the longitude λ and the colatitude θ, $-\pi < \lambda \leq \pi$, $0 \leq \theta \leq \pi$. The colatitude measures the angle to the north pole (by convention $(0, 0, 1)$ in Cartesian coordinates). We use colatitude instead of latitude (which measures the angle to the equatorial plane), because the resulting formulas are shorter. The longitude measures the angle in the xy-plane. Points on D are again identified using polar coordinates with radius r and angle φ, $0 \leq r \leq 1$, $-\pi < \varphi \leq \pi$.

The problem of mapping the sphere onto the disc is one of the classical areas of map projection, and the methods discussed in this section are well known in that field. In the following sections, all methods map the north pole to the center of the unit disc, set the polar angle $\varphi = \lambda - \pi/2$, and compute radius r as a function of the colatitude θ. We will discuss only this radius function for each method.

Only a subset of the mappings covered here can map the whole sphere to the unit disc; others are restricted to a hemisphere. By shifting the north pole of the sphere to another point and suitably recomputing longitude and colatitude, other projection centers can be chosen. In Section 4, we will use the south pole as an additional projection center to cover both north and south hemispheres. For this case, the new colatitude is simply $\pi - \theta$, and the longitude remains unchanged.

The mappings are summarized and compared in Table 2.

3.1. Equal-Area Projection (Lambert Azimuthal)

Lambert designed several important map projections [Snyder 1987], among them the azimuthal equal-area map projection.

Sphere to disc mapping:

$$r = \sin(\theta/2)$$

Disc to sphere mapping:

$$\theta = 2\,\mathrm{asin}(r)$$

When projecting just one hemisphere instead of the whole sphere, an additional scale factor of $\sqrt{2}$ is applied to the radius so that the unit disc is filled.

This mapping can map the whole sphere in a disc. It is an equal-area mapping. Angular distortions increase with distance to the pole.

3.2. Conformal Projection (Stereographic)

The stereographic map projection is a conformal projection that was already known in ancient Greece [Snyder 1987].

	Equal-Area	Conformal	Harmonic Mean	Mixture	Equidistant
Sphere to disc	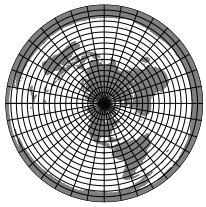		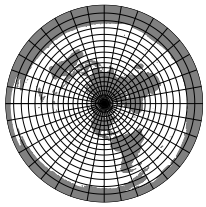		
Hemisphere to disc	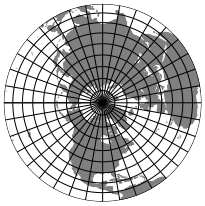	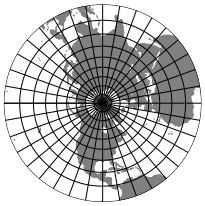	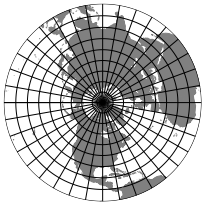	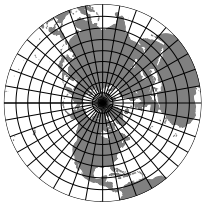	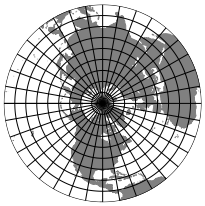
D_A (hemisphere)		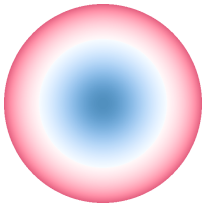			
D_I (hemisphere)	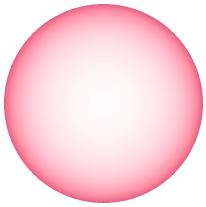				

Table 2. Overview of mappings between a sphere and a disc.

Hemisphere to disc mapping:

$$r = \tan(\theta/2)$$

Disc to hemisphere mapping:

$$\theta = 2\,\mathrm{atan}(r)$$

This mapping cannot be used to map a complete sphere in a disc. It is a conformal mapping. Scale increases with distance from the pole.

3.3. Harmonic Mean of Equal-Area and Conformal Projection (Breusing)

Many attempts have been made to balance the area-preserving qualities of the Lambert azimuthal equal-area projection with the angle-preserving qualities of the stereographic projection, with the goal of arriving at a map projection with only moderate area and angle distortions throughout. Breusing is credited with the idea of using the geometric mean of both projections; Young preferred the harmonic mean over the geometric and arithmetic means and stated that it leads to simpler formulas than the alternatives while being an error-minimizing projection in some sense [Young 1920].

Sphere to disc mapping:

$$r = \tan(\theta/4)$$

Disc to sphere mapping:

$$\theta = 4\,\mathrm{atan}(r)$$

When projecting just one hemisphere instead of the whole sphere, an additional scale factor of $\frac{1}{\sqrt{2}-1}$ is applied to the radius so that the unit disc is filled.

This mapping can map the whole sphere in a disc. It is neither equal-area nor conformal, but both area and angular distortions are moderate.

3.4. Mixture of Equal-Area and Conformal Projection

Instead of using a fixed relation between equal-area and conformal projection, Fong proposes to use a parameterized mixture of both [Fong 2014]. The tradeoff between area and angular distortions can be chosen using a parameter $\beta \in [0, 1]$, with $\beta = 0$ choosing the stereographic projection and $\beta = 1$ choosing the Lambert azimuthal equal-area projection. Fong applied this idea to the whole sphere, which lead to difficulties since the stereographic projection requires an infinite plane to map the complete sphere; in his version, the parameter β can only approach zero, but not become zero. We restrict the mixed projection to the hemisphere instead and can, therefore, use simpler formulas that furthermore do not impose a restriction on β.

Hemisphere to disc mapping:

$$r = \frac{\sqrt{1+\beta}\tan(\theta/2)}{\sqrt{1+\beta\tan^2(\theta/2)}}$$

Disc to hemisphere mapping:

$$\theta = 2\,\mathrm{atan}\left(\frac{r}{\sqrt{1+\beta(1-r^2)}}\right)$$

For $\beta = 0$, $r = \tan(\theta/2)$ and $\theta = 2\,\mathrm{atan}(r)$, thus this mapping becomes the stereographic mapping. For $\beta = 1$, $r = \frac{\sqrt{2}\tan(\theta/2)}{\sqrt{1+\tan^2(\theta/2)}} = \sqrt{2}\sin(\theta/2)$ and $\theta = 2\,\mathrm{atan}(r/\sqrt{2-r^2}) = 2\,\mathrm{asin}(r/\sqrt{2})$, thus this mapping becomes the Lambert azimuthal equal-area mapping in its hemisphere variant.

This mapping cannot map the whole sphere in a disc. It can be equal-area (for $\beta = 1$) or conformal (for $\beta = 0$) and balances area against angular distortions for $0 < \beta < 1$.

3.5. Equidistant Projection

The equidistant map projection has been known for many centuries; its origin cannot be clearly identified [Snyder 1987]. Its main features are its simplicity and the preservation of distances measured from the center of the projection. Its area and angular distortions fall between those of the equal-area and conformal projections, thus making this projection another candidate for a compromise between both.

Sphere to disc mapping:

$$r = \theta/\pi$$

Disc to sphere mapping:

$$\theta = r\pi$$

When projecting just one hemisphere, instead of the whole sphere, an additional scale factor of 2 is applied to the radius so that the unit disc is filled.

This projection can map the whole sphere in a disc. It is neither conformal nor equal-area, but balances area and angular distortions. Distances to the center are preserved.

4. Mappings between Sphere and Square

For projecting a sphere onto a square, there are essentially two layout options, described in the following sections.

Hemisphere to disc mapping	Lambert	Stereographic	Harmonic Mean	Mixture	Equidistant
Disc to square mapping	Shirley	Conformal	Elliptical	Squircle	Elliptical
Example map	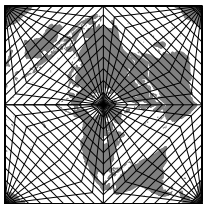	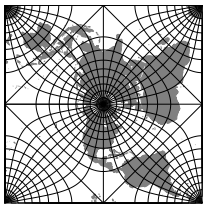	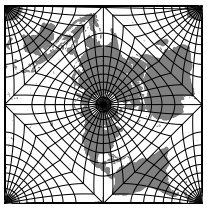	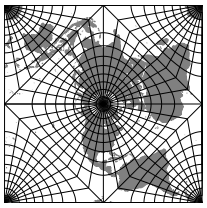	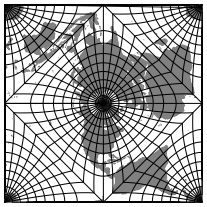
D_A		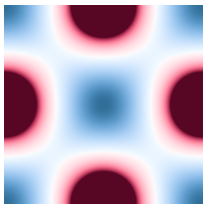		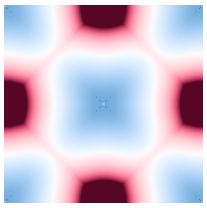	
D_I	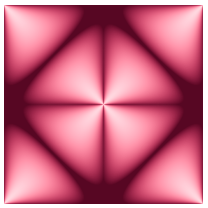			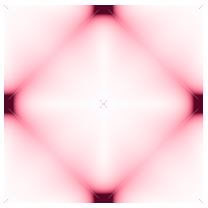	

Table 3. Selected mappings between a sphere and a square in quincuncial layout.

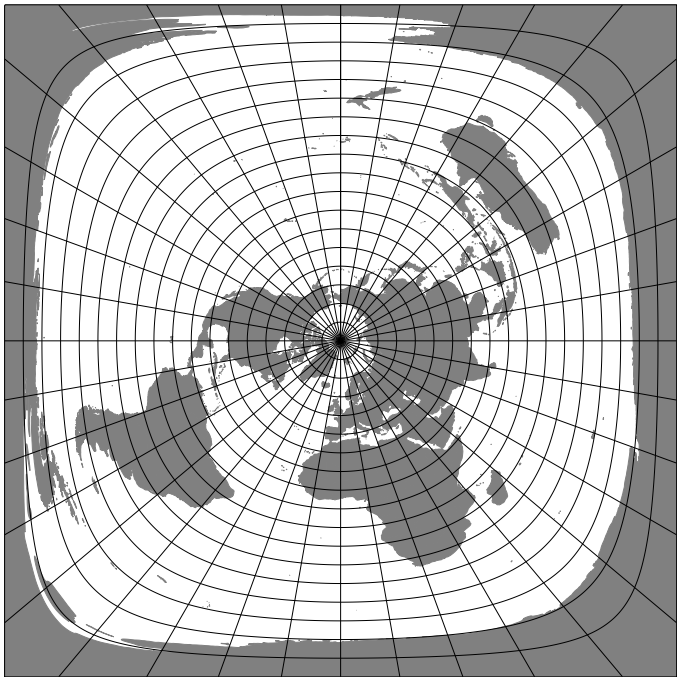

Figure 2. Example map with the south pole of the sphere mapped to the square border. Here the equidistant azimuthal projection was combined with the disc-to-square mapping based on Fernández-Guasti's squircle.

4.1. Pole-at-border Layout

The first layout option projects the whole sphere onto a disc using one of the methods from Section 3 that is capable of this, and then applies one of the methods from Section 2 to map that disc to a square.

In this layout, the sphere point opposite the projection center is mapped to the border of the square. In our examples, the projection center is the north pole, and the south pole is spread across the border. Figure 2 shows an example map.

Obviously, this layout leads to very strong distortions in the region around the point opposite the projection center. This limits its usefulness in applications that require acceptable sampling quality throughout the map, but there are still use cases for this layout, for example in panoramic imaging [Fong 2014].

4.2. Quincuncial Layout

Peirce's quincuncial map projection [Peirce 1879] shown in Figure 3 introduced this layout. It projects each hemisphere onto its own disc, maps these discs to two squares, and then arranges the squares into a single square as depicted in Figure 4. The center part and the four corner parts form a quincunx.

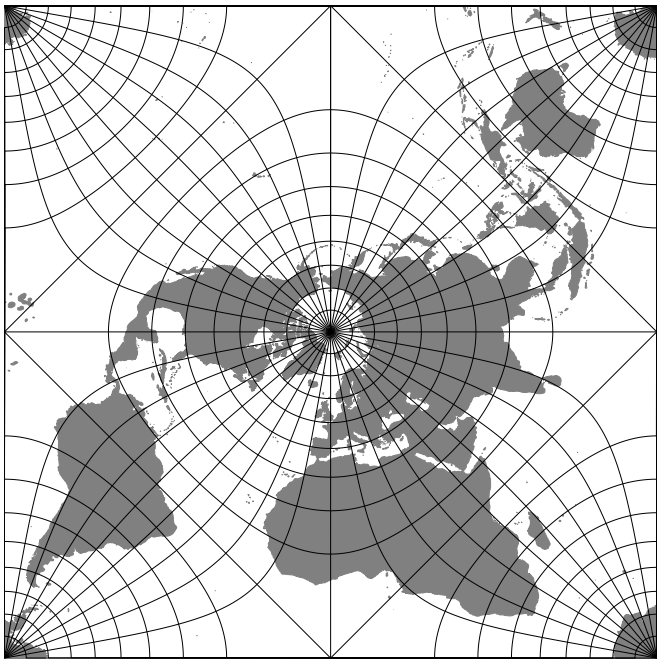

Figure 3. The original quincuncial map by Peirce combines stereographic conformal projection from each hemisphere to a disc, conformal mapping of these discs to two squares, and arrangement of the squares in a quincuncial layout.

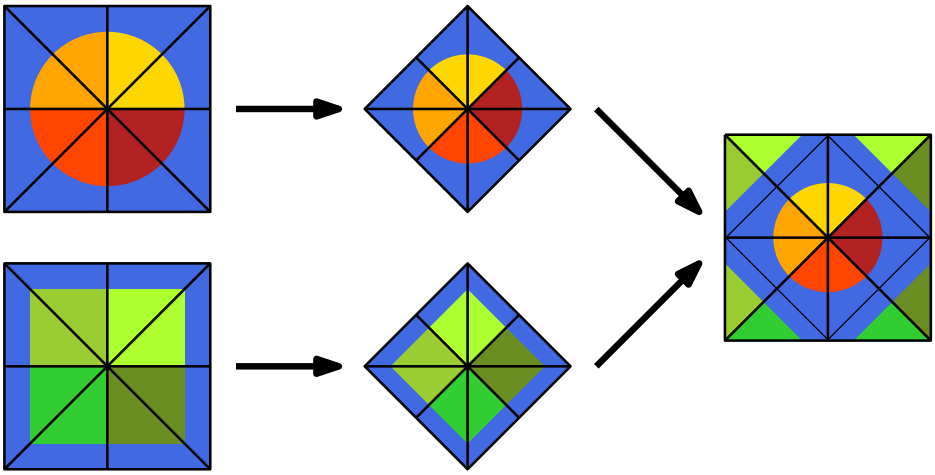

Figure 4. Arrangement of two squares into a new square in quincuncial layout. The second square is mirrored along its borders to fit into the new square.

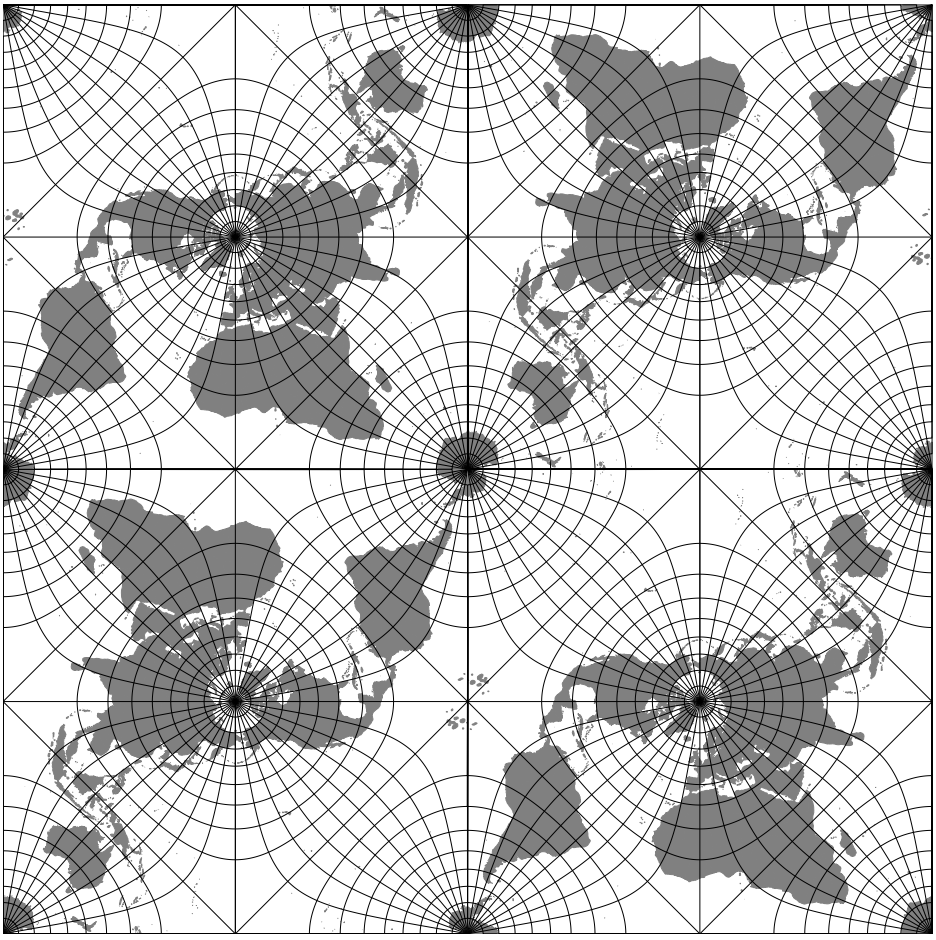

Figure 5. Tiling of the quincuncial layout. The upper-left and lower-right quarters are the original map, the upper-right and lower-left quarters are rotated by $180°$.

The sphere point opposite the projection center is mapped to the four corners of the square. Distortions are much smaller than in the opposite-point-at-border layout. Additionally, the quincuncial layout has the nice property that maps can be tiled, as shown in Figure 5: when leaving the map at any border point except the four corners, in any direction, there is a continuation point where we can re-enter the map without disruption.

The quincuncial layout has been used in computer graphics to represent an octahedron inside a square for the purpose of vector representation [Meyer et al. 2010; Cigolle et al. 2014] or sphere parametrization [Praun and Hoppe 2003] and for the display of panoramic images [German et al. 2007].

To arrange two unit squares into a unit square in quincuncial layout, both must first be rotated by $-45°$ and scaled by $1/\sqrt{2}$. Each quadrant of the second input square R_2 is then mirrored along its border in that quadrant; see Figure 4.

Selected mappings in quincuncial layout are summarized and compared in Table 3. Note that there are methods that map directly between sphere and octahedron or square, without using the disc as an intermediate step. These include Snyder's equal-area map projection for polyhedral globes [Snyder 1992] and Gringorten's square equal-area world map [Gringorten 1972]. Furthermore, Clarberg describes an optimized SIMD implementation of a mapping between sphere and square using Shirley's equal-area mapping and an octahedral layout [Clarberg 2008]. These methods are not discussed in this paper.

5. Analysis

In this section, we derive quality measurements and provide numerical analysis results for all mappings. Note that all results were obtained using IEEE double precision floating-point numbers and computations.

5.1. Distortion Measurements

To evaluate the mapping methods discussed in the preceding sections, we use a standard tool from the field of map projection: Tissot's indicatrix [Snyder 1987].

The idea of the indicatrix is that any map projection maps an infinitesimal circle on the sphere onto an infinitesimal ellipse on the map. This ellipse describes the local characteristics of the map projection. For example, a conformal map projection preserves angles, and the local ellipse will therefore be a circle, but generally not of the same size as the original circle. An equal-area map projection preserves area, and the size ratio of the local ellipse to the original circle will be constant throughout the map, but the axes of the ellipse will have varying orientation and length.

In general, for any pair of lines that intersect at a given point on the sphere, the angle at which they intersect on the map will not be identical (unless the map projection is conformal). The greatest deviation from the correct angle at a given point is called the maximum angular deformation ω.

Both the original circle and the mapped ellipse are infinitesimal, but Tissot's indicatrix allows to compute the ratio between corresponding properties. The most important ellipse properties are the semi-major axis a and the semi-minor axis b. Both are measured relative to the original circle: the identity mapping will result in $a = b = 1$.

For applications in computer graphics, two values derived from a and b are of special interest, since they determine the sampling quality of a map projection:

- *The local area distortion* D_A. The determinant of the Jacobian matrix of a mapping gives the local scale factor s, which can also be determined numerically as $s = ab$. In a strict sense, s must be 1 everywhere on the map for the mapping to be truly area-preserving, but usually source and destination have different areas, and an equal-area mapping will have a constant scale factor representing

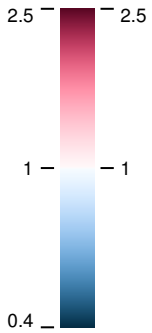

Figure 6. Color map for D_A and D_I in Tables 1, 2, 3 and Figure 7. D_A (left scale) can deviate upward or downward from the ideal value 1, with direction of the deviation encoded in hue. D_I (right scale) can only deviate upward from 1, where it uses the same color encoding as D_A.

the ratio R of destination and source areas, e.g. $s \equiv 4/\pi$ for equal-area mappings from disc to square. We therefore use $D_A = ab/R$ as a measurement of local area distortion.

- *The local isotropy distortion* D_I. The ratio of a and b is a measurement for the isotropy distortion: $D_I = a/b$. The ideal value is 1. Larger anisotropy typically leads to degraded sampling quality in computer graphics applications. Note that conformal maps have $D_I \equiv 1$, but $D_I \equiv 1$ does not imply that a map is conformal: ω might still be larger than zero locally.

These two distortion measurements are color-coded using a color map generated with the methods described by Wijffelaars et al. [Wijffelaars et al. 2008] as shown in Figure 6; they are displayed for all relevant mappings in Tables 1, 2, and 3.

Table 1 shows that for mappings between disc and square, D_A tends to increase strongly in the corners of the square, except for the radial stretching method and, of course, Shirley's equal-area mapping. In fact, D_A grows indefinitely in the corners for Fernández-Guasti's squircle method, elliptical arc mapping, and conformal mapping, with conformal mapping showing the largest errors and affected areas. D_I is strongest at the square diagonals for the radial stretching mapping and Shirley's equal-area mapping, but it does not grow indefinitely for these methods. Fernández-Guasti's squircle method and elliptical arc mapping show indefinitely growing D_I values in the corners of the square. For conformal mapping, $D_I \equiv 0$ as expected.

Interestingly, Shirley's equal-area mapping exhibits the lowest D_I measurements of the non-conformal mappings. It is therefore a good candidate if its discontinuity at the square diagonals is acceptable for the application. On the other hand, Fernández-Guasti's squircle method and elliptical arc mapping provide small D_A and D_I values for the largest part of the square, as can also be seen by looking at the mapped teapot shapes; if an application is mainly interested in the interior of the square and not its corners, these methods are good candidates.

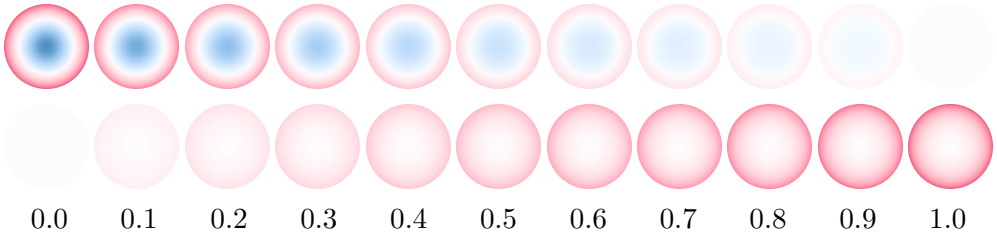

Figure 7. D_A (top) and D_I (bottom) of the method described in Section 3.4, for varying β.

Table 2 shows that the harmonic mean, mixture, and equidistant mappings all provide good compromises in terms of D_A and D_I when compared to the equal-area and conformal mappings. We used $\beta = 0.4$ for the mixture method since it delivers the best compromise; see Figure 7. Still, the harmonic mean method might be preferable if an adjustable error tradeoff is not required.

Table 3 shows only a small subset of the many possible quincuncial combinations of methods. The distortions introduced by sphere/disc and disc/square mappings combine. Compromises between equal-area and conformal mappings still exhibit relatively large values for D_A and D_I at the corners of the inner square, mainly caused by the disc/square mapping. For some applications, it is possible to position these four points in regions of low interest, e.g. oceans for applications that visualize Earth landmass data.

5.2. Precision Measurements

We tested the numerical precision of our implementation by placing a uniform grid on the square map, applying inverse mapping to each grid point to obtain coordinates in the original domain (disc or sphere), and then mapping these coordinates first to the map and then back again. For each obtained point in the original domain, we then have a distance to the point resulting from forward and inverse transformation. The maximum distance is the error measurement.

The mappings between disc and square all have very low errors. Measured on Earth's equatorial disc, the distances are in the micrometer range or below, with two exceptions: Fernández-Guasti's squircle mapping has an error in the millimeter range, and conformal mapping has an error in the meter range. Of course, these are implementation dependent, but we did not arrive at lower distances for the conformal mapping when using different numerical libraries for the computation of F and cn.

The errors of mappings between sphere and square are dominated by the errors of the disc/square mappings used. On an Earth-sized sphere, they are again mostly in the micrometer range, except when Fernández-Guasti's squircle mapping or conformal mapping are used, in which case errors in the millimeter (squircle) or meter range (conformal) occur.

6. Conclusion

This paper gives an overview of mappings between a disc and a square, between a sphere and a disc, and (by composition) between a sphere and a square. It provides ready-to-implement formulas for both the forward and inverse mappings, and it analyzes all mappings using distortion measurements that are relevant for applications in computer graphics.

Since requirements in terms of mapping properties strongly depend on the application area, general recommendations cannot be made. Instead, this paper provides analysis results intended to help pick the right mapping for a given application.

Acknowledgements

The polygonal world map data used in maps throughout this paper is provided by Bjorn Sandvik, http://thematicmapping.org/downloads/world_borders.php, license CC BY-SA 3.0.

References

CIGOLLE, Z. H., DONOW, S., EVANGELAKOS, D., MARA, M., MCGUIRE, M., AND MEYER, Q. 2014. A survey of efficient representations for independent unit vectors. *Journal of Computer Graphics Techniques 3*, 2 (April), 1–30. URL: http://jcgt.org/published/0003/02/01/. 5, 15

CLARBERG, P. 2008. Fast equal-area mapping of the (hemi)sphere using SIMD. *Journal of Graphics, GPU, and Game Tools 13*, 3, 53–68. URL: http://dx.doi.org/10.1080/2151237X.2008.10129263. 16

FERNÁNDEZ-GUASTI, M. 1992. Classroom notes: Analytic geometry of some rectilinear figures. *Int. J. Mathematical Education in Science and Technology 23*, 6, 895–913. URL: http://dx.doi.org/10.1080/0020739920230607. 5

FLOATER, M. S., AND HORMANN, K. 2005. Surface parameterization: a tutorial and survey. In *Advances in Multiresolution for Geometric Modelling*, Mathematics and Visualization. Springer, New York, 157–186. URL: http://dx.doi.org/10.1007/3-540-26808-1_9. 2

FONG, C. 2014. An indoor alternative to stereographic spherical panoramas. In *Proc. Bridges 2014: Mathematics, Music, Art, Architecture, Culture*, 103–110. URL: http://archive.bridgesmathart.org/2014/bridges2014-103.html. 1, 5, 10, 13

FONG, C., 2015. Analytical methods for squaring the disc. http://arxiv.org/abs/1509.06344. Accessed: 2015-10-06. 2, 6

GERMAN, D. M., D'ANGELO, P., GROSS, M., AND POSTLE, B. 2007. New methods to project panoramas for practical and aesthetic purposes. In *Proc. Computational Aesthetics in Graphics, Visualization, and Imaging*, Eurographics Association, Aire-la-Ville, Switzerland. URL: http://dx.doi.org/10.2312/COMPAESTH/COMPAESTH07/015-022. 1, 15

GREENE, N. 1986. Environment mapping and other applications of world projections. *IEEE Computer Graphics and Applications 6*, 11 (Nov.), 21–29. URL: http://dx.doi.org/10.1109/MCG.1986.276658. 1

GRINGORTEN, I. I. 1972. A square equal-area map of the world. *Journal of Applied Meteorology 11*, 5, 763–767. URL: http://dx.doi.org/10.1175/1520-0450(1972)011<0763:ASEAMO>2.0.CO;2. 16

HEIDRICH, W., AND SEIDEL, H.-P. 1998. View-independent environment maps. In *Proc. ACM SIGGRAPH/EUROGRAPHICS Workshop on Graphics Hardware*, ACM, New York, 39–ff. URL: http://dx.doi.org/10.1145/285305.285310. 1

LEE, L. 1976. Conformal projections based on jacobian elliptic functions. *Cartographica 13*, 1, 67–101. URL: http://dx.doi.org/10.3138/X687-1574-4325-WM62. 6

MEYER, Q., SÜSSMUTH, J., SUSSNER, G., STAMMINGER, M., AND GREINER, G. 2010. On floating-point normal vectors. *Computer Graphics Forum 29*, 4, 1405–1409. URL: http://dx.doi.org/10.1111/j.1467-8659.2010.01737.x. 15

NOWELL, P., 2005. Mapping a square to a circle. http://mathproofs.blogspot.com/2005/07/mapping-square-to-circle.html. Accessed: 2015-10-06. 5

PEIRCE, C. 1879. A quincuncial projection of the sphere. *American Journal of Mathematics 2*, 4, 394–396. URL: http://dx.doi.org/10.2307/2369491. 6, 13

PRAUN, E., AND HOPPE, H. 2003. Spherical parametrization and remeshing. *ACM Trans. Graph. 22*, 3 (July), 340–349. URL: http://dx.doi.org/10.1145/882262.882274. 15

ROŞCA, D. 2010. New uniform grids on the sphere. *Astronomy & Astrophysics 520*, A63. URL: http://dx.doi.org/10.1051/0004-6361/201015278. 4

SHIRLEY, P., AND CHIU, K. 1997. A low distortion map between disk and square. *Journal of graphics tools 2*, 3, 45–52. URL: http://dx.doi.org/10.1080/10867651.1997.10487479. 1, 4

SHIRLEY, P., AND CLINE, D., 2011. Improved code for concentric map. http://psgraphics.blogspot.de/2011/01/improved-code-for-concentric-map.html. Accessed: 2016-03-18. 2, 4

SLOAN, P.-P., LUNA, B., AND SNYDER, J. 2005. Local, deformable precomputed radiance transfer. *ACM Trans. Graph. 24*, 3 (July), 1216–1224. URL: http://dx.doi.org/10.1145/1073204.1073335. 1

SNYDER, J., AND MITCHELL, D., 2001. Sampling-efficient mapping of spherical images. http://research.microsoft.com/en-us/um/people/johnsny/papers/spheremap_tr.pdf. Microsoft Research Technical Report. 2

SNYDER, J. 1987. *Map projections—a working manual*, vol. 1395 of *Professional Paper*. US Geological Survey. 8, 11, 16

SNYDER, J. 1992. An equal-area map projection for polyhedral globes. *Cartographica 29*, 1, 10–21. URL: http://dx.doi.org/10.3138/27H7-8K88-4882-1752. 16

STARK, M. M. 2009. Fast and stable conformal mapping between a disc and a square. *Journal of Graphics, GPU, and Game Tools 14*, 2, 1–23. URL: http://dx.doi.org/10.1080/2151237X.2009.10129277. 7

WIJFFELAARS, M., VLIEGEN, R., VAN WIJK, J. J., AND VAN DER LINDEN, E.-J. 2008. Generating color palettes using intuitive parameters. *Computer Graphics Forum 27*, 3, 743–750. doi:10.1111/j.1467-8659.2008.01203.x. 17

YOUNG, A. E. 1920. *Some Investigations in the Theory of Map Projections*. Royal Geographical Society, London. URL: http://www.archive.org/details/cu31924029951401. 10

Index of Supplemental Materials

The supplementary material found at http://www.jcgt.org/published/0005/02/01/code.zip consists of C++ source code implementing all mapping and analysis methods, licensed under the MIT/Expat license. See included README file for an overview.

Author Contact Information

Martin Lambers
Computer Graphics Group
University of Siegen
Hölderlinstraße 3
57076 Siegen
martin.lambers@uni-siegen.de

Martin Lambers, Mappings between Sphere, Disc, and Square, *Journal of Computer Graphics Techniques (JCGT)*, vol. 5, no. 2, 1–21, 2016
http://jcgt.org/published/0005/02/01/

Received:	2015-11-05		
Recommended:	2016-03-15	Corresponding Editor:	Peter Shirley
Published:	2016-04-15	Editor-in-Chief:	Marc Olano